

# PLANNED TESTS OF THE EQUIVALENCE PRINCIPLE WITH A CRYOGENIC TORSION PENDULUM

E. C. Berg, W. D. Cross, and R. D. Newman  
Department of Physics and Astronomy  
University of California at Irvine,  
Irvine, CA 92697-4575, USA  
email: rdnewman@uci.edu

P. E. Boynton, M. W. Moore, and J. H. Steffen  
Department of Physics  
University of Washington  
Seattle, WA 98195-1560, USA  
email: boynton@dirac.phys.washington.edu

## 1 Introduction

Since the work of Eötvös [1], the torsion pendulum has been used with progressively increasing sensitivity to search for differential acceleration of materials with differing composition in the gravitational field of source masses at various ranges [2,3,4,5,6,7].

The torsion pendulum is extraordinary in its ability to measure extremely weak slowly varying forces, and hence has been the instrument of choice for most tests of the equivalence principle (EP) for the last century. However, it has nearly reached the limits of its abilities when operated at room temperature. The logical next step is to operate torsion pendulums at cryogenic temperatures.

### 1.1 Advantages of a cryogenic pendulum

**Low thermal noise** Thermal noise torque driving a pendulum is proportional to  $\sqrt{k_B T/Q}$  and is thus reduced directly by an order of magnitude through operation at 2K, and by an additional order of magnitude due to the greatly increased Q possible at low temperature.

**Frequency stability.** A promising way to determine the strength of the interaction of a pendulum with an external field is to measure the change that the interaction produces in the pendulum's torsional oscillation frequency. However, this method is severely limited at room temperature by systematic error and random noise in the oscillation frequency arising from temperature variation of the pendulum and its torsion fiber. This problem is greatly reduced at low temperature, because the temperature dependence of the fiber's shear modulus and of the pendulum's dimensions becomes very small, and also because of the excellent temperature control that may be maintained at low temperature.

**Highly effective magnetic shielding** A thin lead shield wrapped around the instrument's vacuum chamber in its cryogenic environment pins magnetic field lines, isolating the pendulum from changes in magnetic field as the orientation of a source mass is varied.

**Ultrahigh vacuum** A very high vacuum may be easily attained in the pendulum's environment, using a charcoal "cryopump" near the pendulum to supplement an ion pump operating at room temperature.

## 2 Pendulum operation mode

A difference  $\Delta a$  in horizontal acceleration of a pair of test mass materials suspended symmetrically on a torsion pendulum is reflected in a torque  $N(\theta) = N_0 \sin(\theta)$ , where  $\theta$  is the angular orientation of the pendulum relative to a field source and the peak torque is  $N_0 = p_c \Delta a$ . Here  $p_c$  is the “composition dipole moment” of the pendulum:  $\vec{p}_c = \int \rho \vec{r} dV$ , where  $\rho$  is the density of one of the two test mass materials. The ratio of the torque amplitude  $p_c \Delta a$  to the pendulum’s torsion constant  $\kappa$  gives a dimensionless measure of the signal:  $\epsilon = (p_c/k) \Delta a$ .

There are three distinct modes in which the pendulum may be used to measure  $\epsilon$ , as discussed by Paul Boynton [8] whose University of Washington group developed two of them. The modes differ dramatically in their relative sensitivity to two major sources of systematic and random error: temperature variation and tilt.

**Deflection method.** Here the signal is the displacement  $\Delta\theta$  of the pendulum from its equilibrium position, related to  $\epsilon$  by  $\Delta\theta = \epsilon$  for small  $\epsilon$ . The pendulum remains nearly stationary either relative to a fixed instrument, or to a continuously rotating instrument as in the method pioneered by the “Eot-Wash” group [7] also at the University of Washington. A major advantage of the continuous rotation variant of the deflection method is its ability to vary the orientation of the pendulum relative to a field source without stressing the torsion fiber. Both variants of the deflection method are very sensitive to instrument tilt and to temperature variation, putting severe demands on the control of these environmental factors.

**Frequency method.** Here the signal is a shift in the torsional oscillation frequency of the pendulum, given for small  $\epsilon$  by  $\frac{\Delta\omega}{\omega} = \frac{J_1(A)}{A} \epsilon$  where  $A$  is the amplitude in radians of the pendulum’s oscillation, and  $J_1$  is a Bessel function. Optimal signal/noise is achieved for an amplitude  $A=1.841$  radians. Use of this method in the search for anomalous forces was pioneered by Boynton’s group. With this method, systematic error arising from instrument tilt is very small compared to the deflection method – a very significant advantage, since instrument tilt associated with varying floor loading or heating is one of the most troublesome error sources in gravity experiments using pendulums. A serious problem with the frequency method however is its sensitivity to temperature variation, which limits its capability when operating at room temperature.

**Second harmonic method.** Here the signal is a second harmonic distortion of the pendulum’s oscillation:  $\theta(t) = A \cos(\omega t) + \frac{2}{3} J_2(A) \epsilon \cos(2\omega t) + \dots$ , in response to a torque  $N(\theta) = N_0 \cos(\theta)$  where again  $\epsilon \equiv N_0/k$ . This method, developed by our University of Washington authors, is extraordinarily insensitive to temperature variations and is even more insensitive to tilt than is the frequency method. A drawback of this method however is that it can not take full advantage of the reduced thermal noise of a cryogenic pendulum. For additive noise in the crossings, the second harmonic method yields a signal-to-noise ratio that can be one to two orders of magnitude less favorable than that of the frequency method under ideal conditions.

**Choice of method.** The temperature sensitivity problem of the frequency method may be overcome if the pendulum is operated at low temperature, making this the method of choice.

## 3 The EP test program: accessible parameter space

Ultimately, satellite-based tests of the EP promise far greater sensitivity than can be achieved with a terrestrial torsion pendulum, if an equivalence violation is assumed to be associated with a force of infinite range, but a cryogenic terrestrial torsion pendulum can improve upon current existing limits. Furthermore satellite-based tests have greatly reduced sensitivity to an equivalence violation arising from possible non-Newtonian interactions with ranges below about one hundred kilometers.

Such deviations from Newtonian behavior can be characterized by a two-body potential energy of the form

$$V_{12} = \frac{-Gm_1m_2}{r} \left(1 + \alpha_{12}e^{-r/\lambda}\right) \quad (1)$$

where  $\lambda$  is the range of this putative new interaction and  $\alpha_{12}$  is its strength. The notation  $\alpha_{12}$  reflects a possible composition dependence of the interaction strength, which may be made explicit in terms of “charges”  $q$ :

$$V_{12} = \frac{-Gm_1m_2}{r} \left[1 + \alpha \left(\frac{q}{\mu}\right)_1 \left(\frac{q}{\mu}\right)_2\right] e^{-r/\lambda} \quad (2)$$

where  $(q/\mu)_i$  is the ratio for mass  $i$  of its total charge  $q$  to its mass in atomic mass units. Natural candidates for an effective charge include  $B$  (baryon number),  $N-Z$  (neutron excess), or indeed mass (in which case there would be no composition dependence) [9].

We plan to make EP tests with three different field source masses: a laboratory-scale mass, a mountain, and the sun. This allows the exploration of widely different regions in the interaction range parameter  $\lambda$ .

**I.** To probe for relatively short range interactions, a laboratory source mass will revolve at periodic intervals about a fixed torsion pendulum instrument. The source mass in this case will be a 1.4 ton stainless steel mass assembly mounted on an air bearing [10]. The signal will be modulated with a relatively short period, probably about two hours. The pendulum’s housing remains stationary in this mode. The closest distance between elements of the pendulum and of the source mass is more than 20 cm, so that high order couplings between pendulum and source are intrinsically small and may be nulled with high precision.

**II.** To probe with high sensitivity most of the  $\lambda$  parameter range above about 100 meters, the pendulum together with its housing is to be rotated at periodic intervals in the laboratory. Here both an adjacent mountain which rises 724 meters above our experimental site and the earth as a whole serve as source mass. However, the need to rotate the pendulum together with its housing in the lab raises an issue that must be addressed with care. Due to the anelastic properties of the torsion fiber, this instrument rotation causes a small temporary shift in pendulum oscillation frequency which dies away on a mixture of time scales [11]. The magnitude of this effect is inversely proportional to the  $Q$  of the fiber, and hence is reduced by using a fiber with high  $Q$ . Further, if the velocity profile  $\dot{\theta}(t)$  of the instrument’s rotation is precisely the same as it is periodically rotated first from 0 to  $\pi$  and then from  $\pi$  to 0 in a steady state repetition pattern, there should be no effect on the frequency *difference* measured in the two instrument orientations. Such precise rotation control should be achievable using a high precision angular encoder. Nevertheless, fiber anelastic effects may be the limiting factor in this operation mode.

**III.** To probe the  $\lambda$  parameter range above about  $10^{10}$  meters, the sun will be used as source mass, modulated by the rotation of the earth. In this parameter range the projected sensitivity is comparable to that afforded in principle by method II, with the advantage of avoiding the need to rotate the instrument.

Our planned EP test program targets sensitivity to differential test mass acceleration at a level of  $10^{-14}$  cm/s<sup>2</sup>. Figure 1 illustrates with dotted lines the  $2\sigma$  constraints that an instrument with such sensitivity could place on an interaction of the form of equation 2 for the particular case where charge  $q=B$  (baryon number). The figure compares these constraints with those which are potentially achievable with a space-based test such as STEP [12].

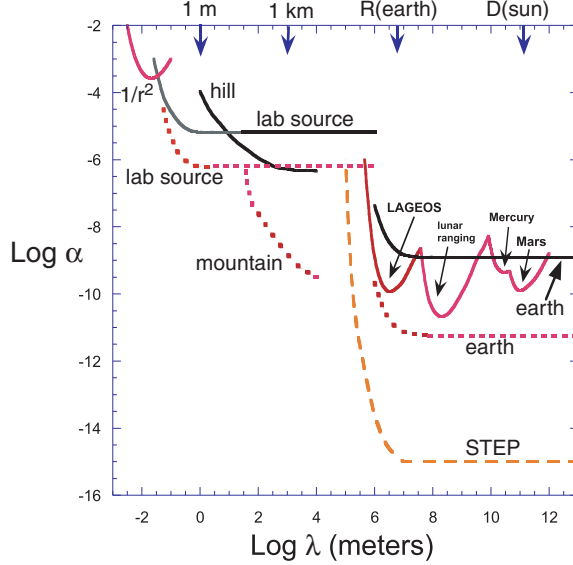


Figure 1: Present and potential  $2\sigma$  constraints on a new force coupling to baryon number (equation 2). The dotted lines are constraints that might be achieved with a torsion pendulum having sensitivity  $\delta a = 10^{-14} \text{cm/s}^2$ . The solid lines labeled “lab source”, “hill”, and “earth”, are existing constraints from the work of the Eot-Wash group [6,7]. The line labeled  $1/r^2$  is a constraint from a previous inverse square law test [13]. The lines labeled LAGEOS, lunar ranging, Mercury, and Mars are from Nordtvedt’s analysis of planetary and satellite orbital data [14]. The dashed line is the projected constraint ability of the proposed satellite EP test STEP.

## 4 Apparatus

### 4.1 The EP pendulum

#### 4.1.1 Pendulum design

The pendulum for the equivalence principle experiments will carry test masses of magnesium and beryllium, materials with good contrast in both N-Z (neutron excess) and B (ratio of baryon number to mass). Two spheres of each material will rest on each of two trays of a fused silica holder (Figure 2). The two trays are connected by a set of four rods. Each ball is to rest on a trio of fused silica hemispheres (not shown) bonded flat side down to a tray. Mirror faces on the lower segment of the pendulum serve for optical position readout. Nominal mass multipole moments of the pendulum vanish for all  $\ell$  through  $\ell = 4$ , excepting  $\ell, m = 4, 4$ , but including  $\ell, 0$  moments. (The  $4, 4$  moment may be nulled by rotating the top layer by  $\frac{\pi}{4}$  relative to the lower layer, at small cost to signal sensitivity.) In the present design the pendulum will carry its eight 12-gram masses at a radius of 2.8 cm, giving a composition dipole moment  $p_c$  (dipole moment of one test mass material only) 121 g cm. It will be suspended by a  $50 \mu\text{m}$  CuBe fiber with torsion constant 1.6 dyn cm/rad, giving a torsional period of 180 seconds with a Q of about 80,000. To achieve symmetry in mass distribution, the magnesium and beryllium balls will be machined to be as close to identical in diameter as possible. The magnesium balls will be of an alloy adjusted to be slightly denser than beryllium. The mass of

the slightly heavier magnesium balls will then be reduced to match that of the beryllium balls by drilling six small holes at the six points where the axes of a Cartesian coordinate system centered on the ball intersect its surface.

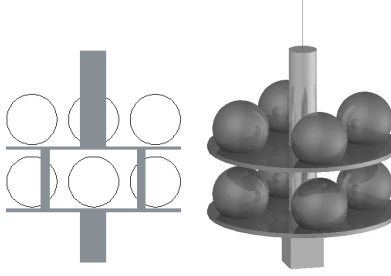


Figure 2: The planned EP test pendulum design with beryllium and magnesium test mass balls on a fused silica carrier. Shown is the current pendulum design and a rendering of an earlier similar design with a central shaft.

#### 4.1.2 Pendulum mass moments

Among the most worrisome sources of systematic error in an EP experiment is the coupling of small (nominally zero)  $m=1$  mass multipole moments of the pendulum to  $m=1$  derivatives of the ambient gravitational field. In principle these moments may be made negligible by an iterative process in which the pendulum’s mass distribution is trimmed after experimentally determining the pendulum’s response to deliberately exaggerated field gradients. This mass trimming will be enabled by a set of split-ring trim masses, one gripping each of the four vertical rods which span the gap between the pendulum’s trays. Vertical adjustment of these trim masses will permit cancelation of residual  $m=1$  moments for  $\ell = 2$  and  $\ell = 3$ . The augmented field gradients will be produced as described in section 4.3 below.

In practice this procedure will be limited not only by error in positioning of the trim masses but also by the reproducibility of the pendulum’s mass distribution at low temperature after a cycle of warming, adjustment, and recooling. Reproducibility in our design will be enhanced through the use of a stable fused silica carrier and spherical test masses which on cooling contract more than the carrier and thus drop slightly on their mount with reproducibility limited only by deviation from sphericity. The placement of the supporting hemispheres will take into account the different contractions of the two materials.

## 4.2 Nulling and monitoring ambient field gradients.

To minimize Newtonian gravitational interactions that can simulate an EP violation signal, it is important not only to trim the pendulum to reduce its low order mass moments, but also to null ambient gravity field gradients as well as possible. This will be done as follows [10]. Before operating the EP pendulum, another pendulum with a deliberately very large  $\ell, m = 2, 1$  moment will operate in its place. This “exaggerated 2,1 moment” pendulum (Figure 4d) will be used to determine the  $\ell = 2, m = 1$  component of the ambient gravitational field. By operating with a set of different pendulum heights it is possible also to determine the  $m=1$  ambient field moments for  $\ell=3$  and even 4. Masses may then be arranged to largely null these field moments.

A remaining problem is the time variation of the ambient field moments – associated with rainfall, changes in underground water table height, atmospheric pressure changes, movement of equipment in the lab, etc. If necessary, we will monitor such gradient variation continuously while the test is in progress. This will be accomplished using a pair of auxiliary “exaggerated 2,1 moment” torsion pendulums located on opposite sides of the EP pendulum, operating at room temperature as independent instruments. The angular orientation of the auxiliary pendulums will be varied at frequent intervals so that each monitors both components of the 2,1 gradient at its location. The average of the gradients read by the two auxiliary instruments will then be a good measure of the gradient at the position of the operating EP pendulum. If we find that the field gradients vary at a level that limits our EP sensitivity, then we plan to implement an active compensation system which will either pump water between stationary tanks or move suspended metal masses along a vertical axis.

### 4.3 The local source mass

For the short-range EP violation search we will use a source mass originally constructed for use in a test of the gravitational inverse square law at distances on the order of 15 centimeters [10,15]. This is a 1.4 ton assembly of stainless steel cylinders (Figure 3) configured to produce a highly uniform horizontal gravitational field at the pendulum position. Expressed in a spherical harmonic expansion, the field due to this source mass has no nominal  $m=1$  contribution for  $\ell = 2$  through 8. This source mass, which is outside the cryogenic environment, will rotate around the pendulum at periodic intervals on its air bearing base.

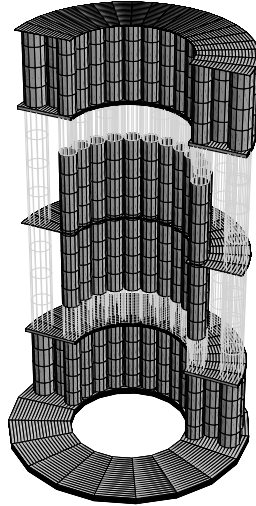


Figure 3: The local source mass. Layers of trays carrying solid stainless steel cylinders are separated by hollow stainless steel tubes in an arrangement which creates an extremely uniform gravitational field at the location of the EP pendulum. Height of the assembly is about 1.8 m.

Residual low-order  $m=1$  moments of this source mass will be detected by measuring their effect on the same “exaggerated 2,1 moment” pendulum that was used to determine the  $\ell = 2$ ,  $m = 1$  component of the

ambient gravitational field. Such measurements made at a set of different vertical positions of the pendulum can be used to measure not only the  $\ell = 2, m = 1$  but also the  $\ell = 3, m = 1$  and in principle even higher  $\ell$   $m=1$  moments of the gravitational field generated by the local source mass [15].

Modifications (Figure 4) of the local source mass, configured to generate at the pendulum's position a deliberately large  $\ell = 2, m = 1$  or  $\ell = 3, m = 1$  field moment, will be used in the procedure described in section 4.1.2 above for trimming the EP pendulum's corresponding multipole moments.

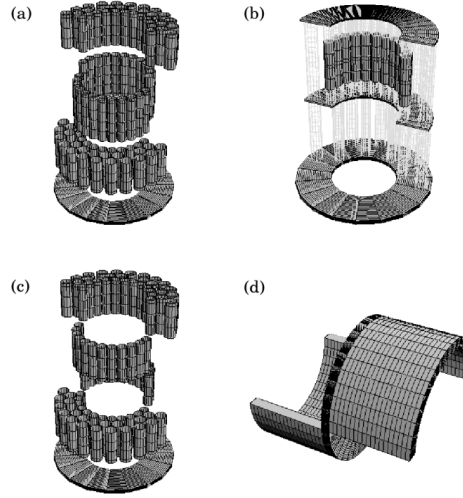


Figure 4: Source mass and pendulum configurations for diagnosing undesired Newtonian gravitational couplings in the EP experiment: (a) Source mass configuration designed to generate a field coupling to a residual  $\ell, m = (2,1)$  mass moment of the EP pendulum. (b) Configuration to couple to a 3,1 mass moment. (c) Configuration coupling to a 4,1 mass moment. (d) Pendulum with deliberate large 2,1 mass moment, to be used in testing for residual (2,1), (3,1), and (4,1) field moments of the source mass of Figure 3. The source masses are about 1.8 meters high, while the pendulum is about 0.1 meters high.

#### 4.4 The cryogenic environment.

The pendulum is to be suspended in a currently operating 3 meter high dewar (Figure 5) holding about 90 liters of liquid helium, which lasts about four days between fills. The dewar may be rotated on precision bearings under computer control to excite torsional oscillations of a pendulum, or to rotate the pendulum's equilibrium position relative to source fields. A vacuum chamber (Figure 6) within the dewar houses the pendulum. Temperature control of the pendulum's environment is maintained in four stages: The vacuum chamber is maintained at 4.2K by the main helium reservoir. Within the vacuum chamber a stage is maintained at 2.0K by a pumped helium pot. A cylindrical shield, with weak thermal coupling to this stage, is held near 2.3K by a PID-controlled heater. The pendulum hangs from yet another stage held near 2.4 by another PID-controlled heater. When working well, control is maintained at this stage to within about 20  $\mu$ K.

## 4.5 Remote underground lab

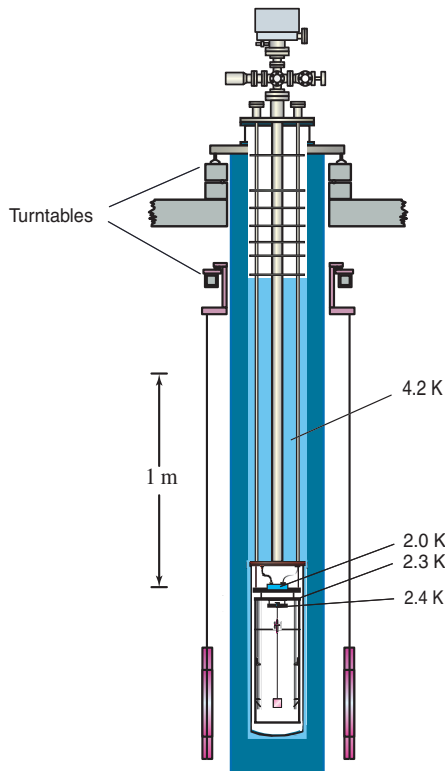


Figure 5: Dewar and cryostat in operation at the Richland site, shown configured for a measurement of the gravitational constant  $G$ .

The experiment will operate in a former Nike missile bunker near Richland, Washington, now converted into the Battelle Gravitational Physics Laboratory (BGPL). The BGPL is located on an arid lands ecology preserve with highly restricted access, on a slope leading to the base of a treeless 1106 meter high basalt mountain. The natural seismic background at this location is unusually low, while the site's 4.8 km distance from the nearest trafficked road makes the cultural vibration contribution also extremely low. It has a modest workshop and library, electronics assembly rooms, hoists, mechanical pumps, and a winched stairway cart for lowering liquid helium storage dewars into the bunker. Seven tons of lead are stacked in a configuration designed to null gravity gradients at the location of our cryostat. Five networked PC computers serve in the lab for experiment control and data logging.

## 5 Performance limitations

We have studied the theoretical limitations on torsion pendulum performance imposed by thermal, seismic, and readout noise sources [16] and by Newtonian gravitational couplings and the effects of nonlinear and anelastic behavior of torsion fibers [17]. Application of these analyses to an earlier EP pendulum design



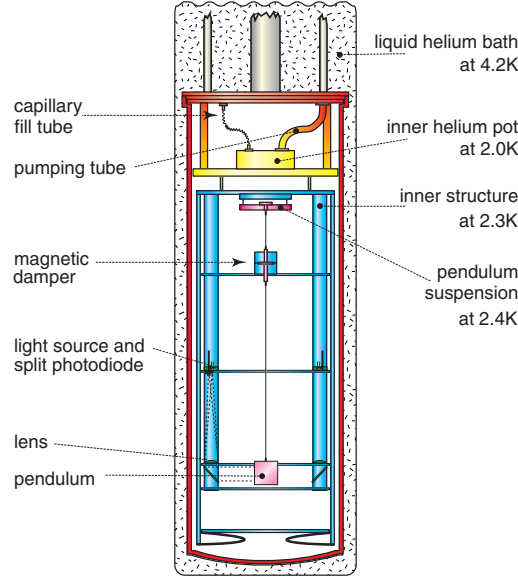


Figure 6: Details of the pendulum environment within the cryostat. Not shown are a recently installed bounce mode damping system and four tiltmeters.

was discussed in reference [18]. In the following we review these limitations for our current EP pendulum design, and conclude that our target of sensitivity to differential accelerations as small as  $10^{-14} \text{cm/s}^2$  is reasonable. However, we also find that the performance of our cryogenic torsion pendulum currently in use for a measurement of the gravitational constant  $G$  falls short of that required for our target EP sensitivity, for reasons yet to be identified.

## 5.1 Expected noise levels

An uncertainty  $\delta\omega$  in the measurement of the EP torsion pendulum's oscillation frequency leads to a corresponding uncertainty in the differential acceleration of the test masses:  $\delta a = \frac{kA}{J_1(A)p_c} \frac{\delta\omega}{\omega}$ , where  $k$  is the pendulum's fiber torsion constant,  $A$  its oscillation amplitude, and  $p_c$  its composition dipole moment. For the parameters of the pendulum discussed here one finds  $\delta a = (0.044 \text{cm/s}^2) \frac{\delta\omega}{\omega}$ . In the following, contributions to  $\frac{\delta\omega}{\omega}$  measurement uncertainty which diminish with the square root of run time are expressed as the uncertainty for a one day run, written as  $\frac{\delta\omega}{\omega} \sqrt{\text{day}}$ . Correspondingly, uncertainties in differential acceleration are expressed as  $\delta a \sqrt{\text{day}}$ .

### 5.1.1 Direct thermal noise

Thermal ( $k_B T$ ) noise contributes a  $\sqrt{Hz}$  uncertainty  $\frac{\delta\omega}{\omega} = \frac{1}{A} \sqrt{\frac{k_B T}{k\omega Q}}$ . For the parameters above and temperature 3K,  $\frac{\delta\omega}{\omega}(\text{thermal}) = 7 \times 10^{-13} \sqrt{\text{day}}$ , or  $\delta a = 3 \times 10^{-14} \text{cm/s}^2 \sqrt{\text{day}}$ .

### 5.1.2 Indirect thermal noise

Variation in the temperature of the torsion fiber introduces noise in the pendulum's oscillation frequency through the temperature dependence  $k(T)$  of its torsion fiber. For the CuBe fiber we expect to use, we have found  $\frac{d[\ln(\omega)]}{dT} \approx 5 \times 10^{-6} K^{-1}$  at 4 K. For our recent data runs in our measurement of the gravitational constant  $G$ , the spectral density of the temperature variation of the fiber suspension point has been typically  $\delta T \approx 5 \times 10^{-5} K/\sqrt{Hz}$  at a signal modulation frequency 0.022 mHz. These data imply a contribution to the pendulum's frequency noise:  $\frac{\delta\omega}{\omega} \approx 8 \times 10^{-13} \sqrt{day}$ , or  $\delta a = 3.5 \times 10^{-14} cm/s^2 \sqrt{day}$ .

### 5.1.3 Readout system noise

The torsional period of the pendulum is determined using an optical lever to record the instants at which the pendulum is at a given angular position. Light from an 870 nm LED is brought to the focal plane of the optical lever with an optical fiber, collimated by a lens, and directed to a mirrored face on the pendulum. The reflected beam is focused to a spot of about 62  $\mu m$  diameter, which traverses a split photodetector as the pendulum rotates. Readout signal/noise ratio could be made almost arbitrarily high by increasing the light intensity, but this intensity must be limited to avoid significant heating of the pendulum. To minimize heating, the light source will be active only during short intervals in which it can give useful information. For a 100  $\mu W$  light source we calculate a pendulum frequency noise:  $\frac{\delta\omega}{\omega} \approx 2 \times 10^{-13} \sqrt{day}$ , or  $\delta a = 8 \times 10^{-15} cm/s^2 \sqrt{day}$ .

### 5.1.4 Seismic noise

Rotational components of seismic noise are expected to be the most important components. Little data exists on such noise. The one estimate available to us (data from a site in New Zealand) suggests a  $\frac{\delta\omega}{\omega}$  contribution at our pendulum frequency noise on the order of  $\frac{\delta\omega}{\omega} \approx 6 \times 10^{-13} \sqrt{day}$ , or  $\delta a \approx 3 \times 10^{-14} cm/s^2 \sqrt{day}$ . This value is the most uncertain in our expected noise budget.

### 5.1.5 Combined noise levels.

The quadrature sum of the noise levels discussed so far is about  $\frac{\delta\omega}{\omega} \approx 1.2 \times 10^{-12} \sqrt{day}$ , or  $\delta a = 5 \times 10^{-14} cm/s^2 \sqrt{day}$ . This assumes all these noise sources have a constant power density (white noise).

### 5.1.6 Instrument tilt

Tilt of the pendulum's environment is likely to be correlated with a modulated signal of interest, and can be a significant problem, even though the frequency method is relatively insensitive to tilt. With our highly asymmetric "G" pendulum we measure a tilt sensitivity  $\frac{\delta\omega}{\omega} = 7 \times 10^{-5}/rad$ , while a symmetric room temperature pendulum currently used for an EP test has an even lower sensitivity:  $\frac{\delta\omega}{\omega} = 5 \times 10^{-6}/rad$ . With an assumption that tilt can be monitored and controlled at an integrated level  $10^{-8}$  radians, the lower of these sensitivities implies a maximum signal error  $\frac{\delta\omega}{\omega} = 5 \times 10^{-14}$  or  $\delta a = 2 \times 10^{-15} cm/s^2$  (an error that need not decrease with run time). In preparation for the EP test we have equipped our instrument with a set of four tilt meters (two for each axis), which operate near the torsion pendulum within its vacuum chamber in the cryogenic environment to ensure that the measured tilt is representative of that experienced by the pendulum's immediate support framework (Figure 7).

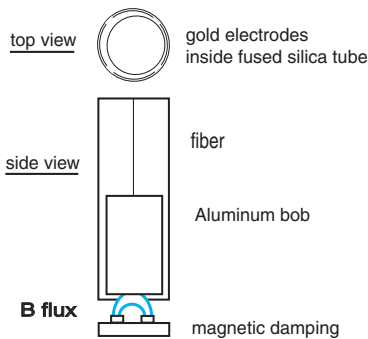


Figure 7: Design of the four tiltmeters installed in the pendulum’s cryogenic environment.

## 5.2 Empirical noise experience in measuring G

Extensive data has been accumulated in a measurement of G using a cryogenic torsion pendulum. The pendulum used is a thin 11 gram fused silica plate suspended in a vertical plane. Three torsion fibers have been used in the course of this work: a  $20\ \mu\text{m}$  diameter CuBe fiber used “as drawn”, a similar fiber that was heat treated, and a  $25\ \mu\text{m}$  diameter Al5056 fiber as drawn. Frequency noise associated with each of these fibers has varied with time, but the “as drawn” CuBe fiber appears to give the best performance. The noise levels when scaled to indicate the frequency noise we would experience with the planned EP pendulum suggest a differential acceleration sensitivity  $\delta a$  ranging from about  $400 \times 10^{-14} \text{cm/s}^2 \sqrt{\text{day}}$  to about  $1200 \times 10^{-14} \text{cm/s}^2 \sqrt{\text{day}}$ . At best this corresponds to a performance about 80 times worse than would be indicated by the analysis in the previous section, and would allow an EP test with only marginally better sensitivity than current room temperature experiments.

We are making an intensive effort to identify the source(s) of this excess noise. The observed frequency noise has no significant correlation with ambient seismic levels. It appears to have roughly comparable contributions from readout noise (error in zero crossing determination) and from noise which is intrinsic to the motion of the pendulum, such as kT thermal noise. For a fit to the zero crossing times of N consecutive oscillation cycles, error in period measurement from white readout noise is expected to decline as  $N^{-3/2}$  while the contribution from thermal noise should decline only as  $N^{-1/2}$ , providing a tool to distinguish these noise types. Analysis of the bipolar voltage signal associated with the transit of the imaged light spot across the split photodetector indicates that the readout noise is predominantly amplifier noise rather than photon shot noise. Both amplifier and shot noise could be reduced by employing a light source with greater intensity. We have been using an LED light source because of its incoherence and ease of modulation, but are at the limits of the intensity of suitable commercially available LEDs (about  $100\ \mu\text{W}$ ). Superluminescent LEDs offer higher intensity, but have displayed high noise levels in our bench tests. Low coherence length lasers are a possibility that we are exploring.

Observed frequency noise levels for the G pendulum using the three quite different fiber types do not differ by a large factor ( $\approx 2$ ), which suggests that the large excess noise is not intrinsic to the torsion fiber.

For each of the three fiber types the same technique was used to attach them at each end: the fiber is centered in a short segment of 1.5 mm OD aluminum tube, with the inner volume of the tube filled with Stycast 1266 epoxy cured at room temperature. It is possible that this interface of the fiber with its upper mount and with the pendulum is a source of excess noise. We plan to test different attachment methods: (1) soldered attachment, (2) 1266 Stycast epoxy cured at high temperature (said to produce a harder material), (3) epoxy attachment after building up the diameter of the fiber by electroplating with copper or other plating material, and (4) gripping the fiber by pinching it between metal jaws. We also plan to test a sapphire fiber. The smallest diameter sapphire fiber that we have found to be commercially available is about  $70\text{ }\mu\text{m}$ , which is too stiff to be useful. We will attempt to reduce this diameter by polishing with diamond grit, ideally to a diameter of about  $30\text{ }\mu\text{m}$ .

We have explored the possibility that the excess noise is associated with “bounce mode” vertical oscillation of the pendulum as its fiber stretches in response to seismic motion. We adapted our eddy current swing mode damping system so that it also damps bounce mode oscillation. Like the original system, the new system (Figure 8) uses a relatively stiff upper fiber coupled to an electrically conducting disk from which the main torsion fiber hangs, with the disk positioned symmetrically between a pair of ring magnets. Swing mode oscillation of the pendulum is communicated to the disk, from which energy is absorbed by induced eddy currents. In the modified system the upper fiber is mounted to a leaf spring as shown in the figure, allowing the disk to move vertically, and the ring magnets are of different diameters so that the flux linking annular regions of the disk varies as the disk moves vertically, with corresponding eddy current damping. The addition of the bounce mode damping was concurrent with a switch from CuBe to Al5056 fiber, so relative effects of the two changes can not be distinguished, but there was no evident reduction in the observed pendulum frequency noise. This was not surprising, given the lack of observed correlation between pendulum frequency noise and measured ambient seismic noise.

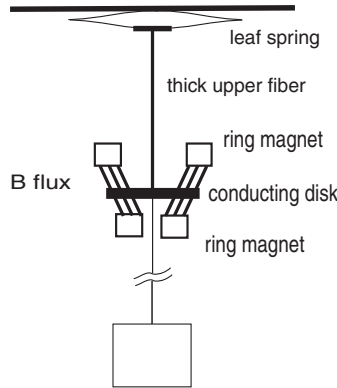


Figure 8: The bounce mode damping system. Magnetic flux linking the damping disk produces eddy currents that damp both horizontal swing and vertical “bounce” pendulum oscillation modes.

There is a possibility that the excess noise may arise from oscillation modes associated with the deliberately large quadrupole moment of the “G” pendulum. To test this possibility we are constructing a pendulum with nominally zero quadrupole moment. This will be used in the tests of various fiber mounting schemes and in the development of an improved optical readout. We remain hopeful that we can achieve EP sensitivity at a level of about  $\delta a = 10^{-14}\text{ cm/s}^2$  for an integration time not more than 100 days. We believe the cryogenic torsion pendulum remains the best hope for achieving such sensitivity for source field ranges

less than tens of kilometers.

## Acknowledgments

We acknowledge the support of the Pacific Northwest National Laboratory, our experimental site host, and particularly thank Roy Gephart of that laboratory. The cryogenic pendulum system was largely developed by Michael Bantel. Many undergraduates have contributed to this work, most recently Henry Choi, Paul Nylander, Jason Siu, and Melissa Tong. This research is funded under National Science Foundation grants PHY-0108937 and PHY-0404514.

## References

- [1] R.V. Eötvös, D. Pekár, and E. Fekete, Ann. Phys. (Leipzig) **68**, 11 (1922).
- [2] P.G. Roll, R. Krotkov, and R.H. Dicke, Annals of Physics **26**, 442 (1964).
- [3] V.B. Braginsky and V.L. Panov, Sov. Phys. JETP **34**, 463 (1972).
- [4] P.E. Boynton, D. Crosby, P. Ekstrom, and A. Szumilo, Phys. Rev. Lett. **59**, 1385 (1987).
- [5] R. Cowsik, N. Krishnan, S.N. Tandon, and S. Unnikrishnan, Phys. Rev. Lett. **64**, 336 (1990).
- [6] Y. Su, B.R. Heckel, E.G. Adelberger, J.H. Gundlach, M. Harris, G.L. Smith, and H.E. Swanson, Phys. Rev. D **50**, 3614 (1994).
- [7] G.L. Smith, C.D. Hoyle, J.H. Gundlach, E.G. Adelberger, B.R. Heckel, and H.E. Swanson, Phys. Rev. D **61**, 022001 (1999).
- [8] P.E. Boynton, Class. Quantum Grav. **17**, 2319 (2000).
- [9] E. Fischbach and C. L. Talmadge, *The Search for Non-Newtonian Gravity*, AIP Press: Springer (1999).
- [10] E.C. Berg, M. K. Bantel, W. D. Cross, T. Inoue, R. D. Newman, J. H. Steffen, M. W. Moore, and P. E. Boynton, in *Proc. 10th Marcel Grossmann Meeting on Recent Developments in Theoretical and Experimental General Relativity, Gravitation and Relativistic Field Theories*, ed. M. Novello, S. Perez-Bergliaffa and R. Ruffini (World Scientific), under review (2002).
- [11] R.D. Newman and M.K. Bantel, Journal of Alloys and Compounds **310**, 233 (2000).
- [12] J. Mester, R. Torii, P. Worden, N. Lockerbie, S. Vitale, and C. W. F. Everitt, Class. Quantum Grav. **18**, 2475 (2001).

- [13] J.K. Hoskins, R.D. Newman, R. Spero, and J. Schultz, Phys. Rev. D **32**, 3084 (1985).
- [14] K. Nordtvedt, in *Testing Relativistic Gravity in Space*, ed C. Lämmerzahl et al, (2000).
- [15] M.W.Moore, A Boudreaux, M. DePue, J. Guthrie, R. Legere, A. Yan, and P.E. Boynton, Class. Quantum Grav. **11**, A97 (1994).
- [16] R.D. Newman, N. Krishnan, M.A. Beilby, M.K. Bantel, E. Siragusa, P.E. Boynton, and A. Goodson, *Proc. 7th Marcel Grossmann Meeting on General Relativity*, ed. R.T. Jantzen et al (World Scientific), 1619 (1996).
- [17] R.D. Newman, M.K. Bantel, and Z.R. Wang, in *Dark Matter in Cosmology, Quantum Measurements, Experimental Gravitation*, ed. R. Ansari et al (Editions Frontieres), 409 (1996).
- [18] R. Newman, Class. Quantum Grav. **18**, 2407 (2001).